

Emergence of superconductivity in heavy-electron materials

Yi-feng Yang (杨义峰)^{a,b,1} and David Pines^{c,d,1}

^aBeijing National Laboratory for Condensed Matter Physics and Institute of Physics, Chinese Academy of Sciences, Beijing 100190, China; ^bCollaborative Innovation Center of Quantum Matter, Beijing 100190, China; ^cDepartment of Physics, University of California, Davis, CA 95616; and ^dSanta Fe Institute, Santa Fe, NM 87501

Contributed by David Pines, November 19, 2014 (sent for review November 3, 2014)

Although the pairing glue for the attractive quasiparticle interaction responsible for unconventional superconductivity in heavy-electron materials has been identified as the spin fluctuations that arise from their proximity to a magnetic quantum critical point, there has been no model to describe their superconducting transition at temperature T_c that is comparable to that found by Bardeen, Cooper, and Schrieffer (BCS) for conventional superconductors, where phonons provide the pairing glue. Here we propose such a model: a phenomenological BCS-like expression for T_c in heavy-electron materials that is based on a simple model for the effective range and strength of the spin-fluctuation-induced quasiparticle interaction and reflects the unusual properties of the heavy-electron normal state from which superconductivity emerges. We show that it provides a quantitative understanding of the pressure-induced variation of T_c in the “hydrogen atoms” of unconventional superconductivity, CeCoIn₅ and CeRhIn₅, predicts scaling behavior and a dome-like structure for T_c in all heavy-electron quantum critical superconductors, provides unexpected connections between members of this family, and quantifies their variations in T_c with a single parameter.

heavy fermion | spin fluctuation | BCS | two-fluid model

Because the unconventional superconductivity found in many heavy-electron materials arises at the border of antiferromagnetic long-range order, it is natural to consider the possibility that its physical origin is its proximity to a quantum critical point that marks a transition from localized to itinerant behavior, and that the associated magnetic quantum critical spin fluctuations provide the pairing glue (1–5), in contrast to conventional superconductors, where phonons provide the pairing glue (6). However, developing a simple physical picture for the behavior of such quantum critical superconductors, including a Bardeen, Cooper, and Schrieffer (BCS)-like expression for their superconducting transition temperature (T_c), has proven difficult. In part, this is because of the unusual normal state from which superconductivity emerges (7–12), and in part it stems from the difficulty in finding a simple model for an effective frequency-dependent attractive quasiparticle interaction that closely resembles that proposed earlier for the cuprates (13–17).

In finding a way to characterize heavy-electron quantum critical superconductivity it is helpful to begin by recalling the principal features of its remarkably similar emergence in two of the best-studied materials, CeCoIn₅ and CeRhIn₅ (18–23). As may be seen in Fig. 1, there are three distinct regions of emergent heavy-electron superconductivity in their pressure–temperature phase diagrams that are defined by a line marking the delocalization cross-over temperature, T_L , at which the collective hybridization of the local moments becomes complete and the Néel temperature, T_N , that marks the onset of long-range antiferromagnetic order of the hybridized local moments.

Region I: $T_c \leq T_L$. Superconductivity emerges from a fully formed heavy-electron state. The general increase in T_c seen with decreasing pressure is cut off by a competing state, quasiparticle localization, so T_c reaches its maximum value at

the pressure, p_L , at which the superconducting and localization transition lines intersect.

Region II: $T_c > T_L$ and T_N . Superconductivity emerges from a partially formed heavy-electron state whose ability to superconduct is reduced by the partially hybridized local moments with which it coexists. The region includes the quantum critical point (QCP) at $T = 0$ that marks a zero temperature transition from a state with partially localized ordered behavior to one that is fully itinerant; this QCP is the origin of the quantum critical spin fluctuations that provide the pairing glue in all three regions (2).

Region III: $T_c \leq T_N$. Partially hybridized local moments are present in sufficient number to become antiferromagnetically ordered at the Néel temperature T_N despite the presence of coexisting remnant heavy electrons that become superconducting at lower temperatures.

The dominance of superconductivity around the QCP supports the idea that the coupling of quantum critical spin fluctuations to the heavy-electron quasiparticles plays a central role, with the resulting induced attractive quasiparticle interaction being maximally effective near it. Importantly, there is direct experimental evidence that these quantum critical fluctuations provide the superconducting glue: Curro et al. (4) find that the spin-lattice relaxation rate, $1/T_1$, to which these give rise, scales with T_c at the pressure at which T_c is maximum, whereas a recent detailed investigation of that scaling (5) explains how this comes about. First, at this “optimal” pressure, T_c scales with the coherence temperature, T^* , that marks the initial emergence of heavy-electron behavior and is determined by the nearest-neighbor exchange interaction between the f -electron local moments (8); second, at this optimal pressure, $1/T_1$ scales with T^* , a scaling behavior that is a unique signature of its origin in quantum critical spin fluctuations.

Significance

Although the pairing glue for the unconventional superconductivity found in heavy-electron materials has been identified as quantum critical spin fluctuations associated with their proximity to antiferromagnetic order, until now we have lacked a simple expression for their superconducting transition temperature, T_c , that explains why T_c changes with pressure, or varies from one material to another. The experiment-based expression proposed here parameterizes the effective frequency-dependent quasiparticle interactions in terms of their unusual normal-state properties; it provides a quantitative explanation of the measured pressure-induced variation in T_c in the “hydrogen atoms” of unconventional superconductivity, CeCoIn₅ and CeRhIn₅, predicts a similar pressure variation for other heavy-electron quantum critical superconductors, and quantifies their variations in T_c with a single parameter.

Author contributions: Y.-f.Y. and D.P. designed research; Y.-f.Y. and D.P. performed research; Y.-f.Y. analyzed data; and Y.-f.Y. and D.P. wrote the paper.

The authors declare no conflict of interest.

¹To whom correspondence may be addressed. Email: yifeng@iphy.ac.cn or david.pines@gmail.com.

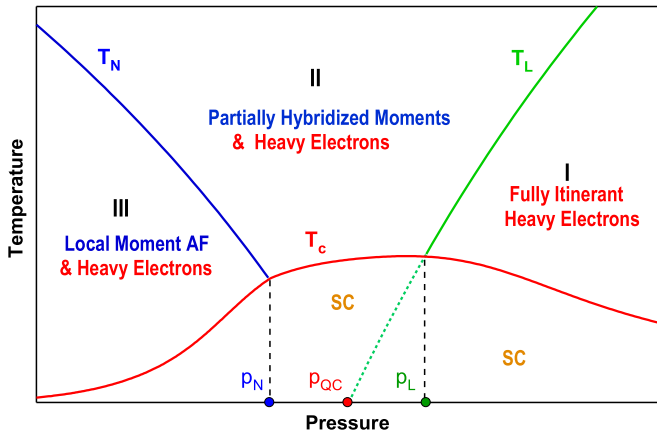


Fig. 1. A phase diagram for heavy-electron superconductors. In region I, only itinerant heavy electrons exist below T_L owing to complete hybridization of the f -moments with background conduction electrons; in region II, collective hybridization is not complete so that heavy electrons coexist with partially hybridized local moments; in region III, these residual moments order antiferromagnetically (AF) at T_N and the surviving heavy electrons become superconducting (SC) at a lower temperature, T_c . The coupling of heavy electrons to the magnetic spin fluctuations emanating from the QCP is responsible for the superconductivity in all regions.

In this paper we use these important scaling results to develop a simple BCS-like phenomenological expression for the superconducting transition temperature, show that it explains the variation of T_c with pressure for both CeCoIn₅ and CeRhIn₅, and offer a detailed prediction for a similar dome-like structure in other quantum critical heavy-electron superconductors.

Phenomenological BCS-Like Model for Heavy-Electron Superconductivity

For phonon-induced superconductivity, BCS found a simple expression for T_c that depended on three quantities (6): the quasiparticle density of states; the average strength, V , of the phonon-induced attractive interaction between quasiparticles; and the average energy range over which it is attractive. Our proposed phenomenological heavy-electron quantum critical magnetic expression involves magnetic analogs of these quantities, all of which can be determined from experiment: $N_F(p, T_c)$, the heavy-electron density of states at T_c ; an effective attraction, $V(p) = \eta k_B T^*(p)$, where $T^*(p)$ is the pressure-dependent interaction between local moments, k_B is the Boltzmann constant, and η is a parameter that measures the relative effectiveness of spin fluctuations in bringing about superconductivity for a given material; and, consistent with the above scaling results, a range of energies over which the quantum critical spin-fluctuation-induced interaction will be attractive that is proportional to T_m^* , the coherence temperature at the pressure p_L , at which T_c is maximum. It takes the form

$$T_c(p) = 0.14 T_m^* \exp\left(-\frac{1}{N_F(p, T_c) V(p)}\right) = 0.14 T_m^* \exp\left(-\frac{1}{\eta \kappa(p)}\right), \quad [1]$$

where we have introduced the dimensionless characteristic coupling strength, $\kappa(p) = N_F(p, T_c) k_B T^*(p)$ and, as discussed below, used experiment to determine the prefactor 0.14.

It is important to note that because experiment shows that the heavy-electron specific heat varies inversely as T^* and grows logarithmically as the temperature is lowered (10, 12), $C/T \sim 1/T^* \ln(T^*/T)$, the density of states, $N_F(p, T_c)$, will exhibit a similar dependence on $T^*(p)$. Because experiment shows that $T^*(p)$

varies monotonically with increasing pressure (Fig. 2B, Inset), without a countervailing $T^*(p)$ dependence in the strength of spin-fluctuation-induced interaction the dimensionless pairing strength would vary monotonically and Eq. 1 could never lead to the dome structure of T_c seen experimentally.

Eq. 1 may be rewritten as

$$\ln \frac{T_c(p)}{T_m^*} = \ln 0.14 - \frac{\eta^{-1}}{\kappa(p)}. \quad [2]$$

For different materials, a plot of the experimental value of $\ln(T_c/T_m^*)$ against $1/\kappa(p)$ therefore provides a test of our BCS-like expression for T_c . As discussed in *Methods*, in the absence of systematic specific heat measurements $\kappa(p)$ may be determined from experiment by using a two-fluid analysis (7–12) to obtain the heavy-electron density of states, N_F ; the resulting values of $\kappa(p)$ for CeCoIn₅ and CeRhIn₅ are given in Fig. 2A. When used to test the validity of Eq. 2, we find, as can be seen in Fig. 2B, that the two materials fall on the same line, a scaling result that provides strong evidence for the validity of our BCS-like equation, whereas the common intercept tells us that $0.14 T_m^*$ is the best choice for the range of the spin-fluctuation-induced attraction for the two compounds.

Our model enables us to predict the maximum effectiveness of the spin-fluctuation-induced interaction for a given material; it is given by

$$\lambda_{\max} = \eta \kappa(p_L) = \ln(0.14 T_m^*/T_c^{\max})^{-1}. \quad [3]$$

We further note that because $\kappa(p)$ is the only pressure-dependent quantity in Eq. 1, our predicted ratio, $T_c(p)/T_c^{\max}$, involves no free parameters and takes the simple form

$$\frac{T_c(p)}{T_c^{\max}} = \exp\left[-\lambda_{\max}^{-1} \left(\frac{\kappa(p_L)}{\kappa(p)} - 1\right)\right]. \quad [4]$$

As may be seen in Fig. 2C and D, when we use the values of $\kappa(p)$ shown in Fig. 2A as input and determine λ_{\max} to be 1.23 for CeCoIn₅ and 0.62 for CeRhIn₅ from experiments at p_L , Eq. 4 provides a remarkably good quantitative explanation of the dome-like structure observed as the pressure is varied in CeCoIn₅ and CeRhIn₅ (18, 19). We note that both $\kappa(p)$ and $T_c(p)$ are peaked at p_L , the pressure at which the delocalization line, T_L , intersects with T_c . Our model successfully explains the decrease in T_c above this pressure as being brought about by the reduction in the heavy-electron density of states produced by the increase in T_L ; below this pressure, the decrease in T_c arises from the reduction in the heavy-electron density of states brought about by the partial localization of the heavy electrons.

Discussion

Encouraged by the above results, we next apply our approach to the emergence of superconductivity in other heavy-electron materials (24–30) for which T^* has been measured and Curro scaling has been established or seems likely to apply. Our results are given in Table 1, where the characteristic dimensionless coupling strength, $\kappa(p_L)$, has been calculated using the two-fluid expression for N_F , and the effectiveness parameter, $\eta = \lambda_{\max}/\kappa(p_L)$, is obtained at the measured (or assumed) optimal pressure, p_L . We call attention to a striking similarity in the values of λ_{\max} shown in Table 1: UPT₃ seems to be a sister element to CeCoIn₅ and PuCoIn₅, even though their superconducting transition and coherence temperatures differ by a factor of five and their superconducting states possess different symmetries. The large value of η found for CeRhIn₅ suggests that in this material the effective interaction, V , could be as large as $3T^*$, and the fact that $\eta > 1$ for

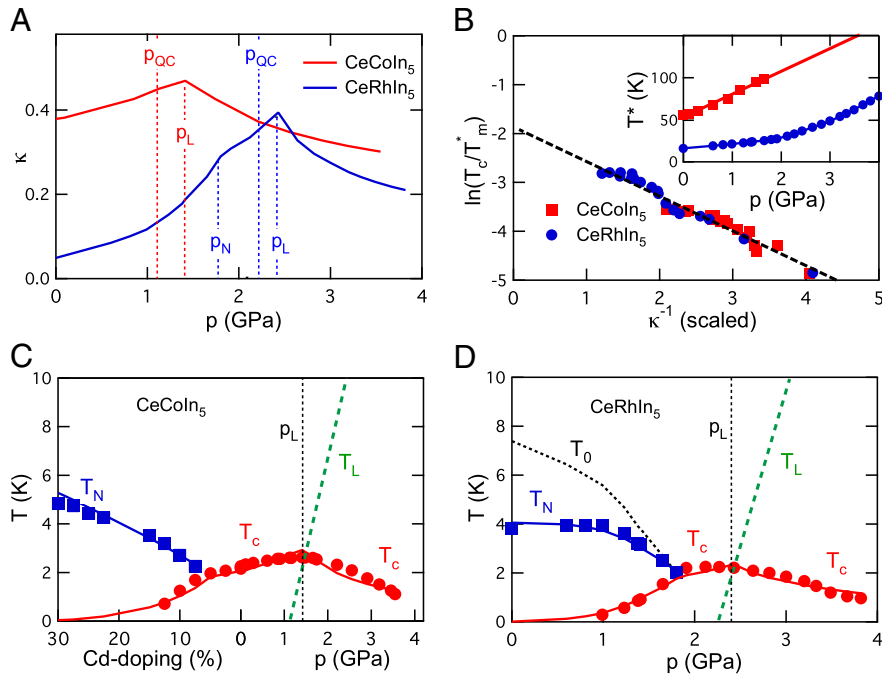


Fig. 2. Comparison of theory and experiment for the ordering temperatures measured in $\text{CeCo}(\text{In}_{1-x}\text{Cd}_x)_5$ and CeRhIn_5 . (A) Pressure variation of the predicted dimensionless pairing strength (*Methods*), $\kappa(p) = k_B T^*(p) N_F(p, T_c)$. (B) Scaling of $\ln(T_c/T_m^*)$ and $\kappa(p)^{-1}$ (scaled) for CeCoIn_5 and CeRhIn_5 . (Inset) The experimental values of $T^*(p)$ that are used to obtain $\kappa(p)$ in both compounds (7, 19). (C) Comparison of the predicted (solid lines) and experimental T_c and T_N in $\text{CeCo}(\text{In}_{1-x}\text{Cd}_x)_5$ and CeCoIn_5 with $\eta = 1.30$ and $\lambda_{\max} = 0.62$ (19, 21). (D) Comparison of the predicted (solid lines) and experimental T_c and T_N in CeRhIn_5 with $\eta = 3.09$ and $\lambda_{\max} = 1.23$ (18).

many materials suggests that the effective attractive interaction is generally somewhat greater than T^* .

Importantly, because there is only a modest variation in $\kappa(p_L)$ as one goes from one material to another, most of the measured variation in $[T_c/T_m^*]_{\max}$ is likely due to variations in the impedance match between the spin-fluctuation spectrum and the heavy-electron Fermi surface that we have parametrized by η . These variations can be explained by changes in effective dimensionality and crystal structure. As Monthoux and Lonzarich emphasized in their seminal papers (16, 17), near two dimensionality and a tetragonal crystal structure are most favorable to superconductivity; their presence in CeRhIn_5 at 2.4 GPa and PuCoGa_5 could explain the relatively large values of η seen for these materials, whereas their absence in CeIn_3 would explain its low value of η and its very low T_c/T_m^* .

CeRhIn_5 at 2.4 GPa and PuCoGa_5 demonstrate how very effective spin fluctuations can be in bringing about superconductivity; their T_c is an appreciable fraction of the effective heavy-electron Fermi energy, $k_B T_c/E_F = 2k_B T_c N_F(T_c)/3$, being 0.016 and 0.013, respectively, fractions large compared with those seen

in the cuprates and very large compared with those found for conventional superconductors. Our model for heavy-electron superconductivity leads to the prediction that the maximal value of the ratio $k_B T_c/E_F$ is ~ 0.03 , about twice the above values.

As a first step toward understanding the microscopic origin of Eq. 1, we can ask whether it is consistent with the anticipated results of a microscopic strong coupling calculation of quantum critical spin-fluctuation-induced superconductivity for heavy-electron materials that takes full account of an experimentally determined frequency-dependent interaction. We find (*Methods*) in the case of CeCoIn_5 , where neutron-scattering experiments yield direct information on the quantum critical spin fluctuation spectrum, that the range of the effective attractive interaction found in microscopic strong coupling calculations is remarkably close to what we propose phenomenologically, and complete consistency is obtained provided the coupling of quasiparticles to the spin fluctuations scales with T^* . This is but a first step, but we hope that this consistency will encourage the development of a complete microscopic derivation of our simple phenomenological BCS-like equation for T_c in which quantum critical

Table 1. T_c , T_m^* , and calculated parameters at the measured or proposed optimal pressure, p_L , for known quantum critical heavy-electron superconductors

	CeRhIn ₅	CeCoIn ₅	CeIrIn ₅	PuCoGa ₅	PuCoIn ₅	Ce ₂ PdIn ₈	Ce ₂ CoIn ₈	CeIn ₃	UPt ₃
p_L , GPa	2.4	1.4	2.2	0	0	0	0	2.8	0
$T_c(p_L)$, K	2.3	2.6	1.05	18.5	2.5	0.7	0.4	0.2	0.5
T_m^* , K	37	92	100	430	100	25	50	80	20
T_c/T_m^*	0.062	0.028	0.011	0.043	0.025	0.028	0.008	0.0025	0.025
$\kappa(p_L)$	0.40	0.48	0.59	0.44	0.49	0.48	0.61	0.74	0.49
λ_{\max}	1.23	0.62	0.39	0.85	0.58	0.62	0.35	0.25	0.58
η	3.09	1.30	0.66	1.94	1.18	1.29	0.57	0.34	1.18
$k_B T_c/E_F$	0.016	0.009	0.004	0.013	0.008	0.009	0.003	0.001	0.008
References	7, 18	11, 19	24, 25	3, 4	26	27	28	29	8, 30

spin-fluctuation superconductivity can be characterized by a range, $\sim 0.14T_m^*$, and a pressure-dependent strength, ηT^* , both of which can be determined directly from experiment.

Another interesting question for future study is whether our phenomenological approach to quantum critical spin-fluctuation-induced superconductivity in heavy-electron materials can be extended to the cuprates and any other unconventional superconductors in which scaling behavior for the spin-lattice relaxation rate with T_c has been seen at or near optimal doping levels.

Methods

Determining the Characteristic Dimensionless Pairing Strength, $\kappa(\rho)$, from Experiment. In the Fermi liquid regime (region I in Fig. 1), where the density of states can be derived from the specific heat measurements and the coherence temperature, $T^*(\rho)$, can be estimated from the resistivity, the dimensionless pairing strength, $\kappa(\rho)$, can be directly determined from experiment, so that our proposed BCS-like Eq. 4 involves no free parameters and could be verified without any further assumptions. However, because the relevant experimental information on the pressure dependence of the specific heat is not yet generally available, to test the applicability of Eq. 4 to heavy-electron materials under pressure we have used the two-fluid model to determine the pressure dependence of the density of states. This procedure has earlier been shown to yield correct specific heat results for a number of heavy-electron compounds (7).

The Delocalization Line, Néel Temperature, and Heavy-Electron Density of States. In the two-fluid model, the three regions in Fig. 1 are determined by the hybridization parameter (7),

$$f(\rho, T) = f_0(\rho) [1 - T/T^*(\rho)]^{3/2}, \quad [5]$$

which quantifies the fraction of f -electrons that become itinerant. The pressure dependence of the hybridization effectiveness, $f_0(\rho)$, discussed below, can be determined from magnetic experiments (cf. ref. 11). For $f_0 > 1$, the cross-over line of complete delocalization temperatures, T_L , in the heavy-electron phase diagram is obtained by setting $f(T_L) = 1$, so that

$$T_L(\rho) = T^*(\rho) [1 - f_0(\rho)^{-2/3}]. \quad [6]$$

For $f_0 < 1$, a fraction of residual local moments always remains and becomes antiferromagnetically ordered at low temperatures. The two-fluid model predicts that the Néel temperature, T_N , is given by:

$$\frac{T_N(\rho)}{T^*(\rho)} = \eta_N [1 - f(T_N, \rho)], \quad [7]$$

where the frustration parameter, η_N , is independent of pressure and found to be 0.14 for CeCoIn₅ and 0.32 for CeRhIn₅ in Fig. 2 C and D.

The heavy-electron density of states in Eq. 1 is obtained in the two-fluid model by assuming that $N_f(T)$ follows the heavy-electron specific heat, according to $N_f(T) = (3/\pi^2 k_B^2) f(T) C_{HE}/T$; experiment shows that the latter grows logarithmically as the temperature is lowered (7, 10, 12), $C_{HE}/T = (k_B \ln 2 / 2T^*) (1 + \ln(T^*/T))$, where the prefactor in C_{HE}/T is determined by requiring the entropy at T^* , $S(T^*) = \int_0^{T^*} dT (C_{HE}/T) = k_B \ln 2$ and is cancelled out in our proposed Eq. 4. The logarithmic growth is cut off by complete delocalization at T_L in region I, superconductivity at T_c in region II, and long-range magnetic order at T_N , or its precursor at T_0 , the temperature at which heavy electrons begin to relocalize before the emergence of hybridized local moment order at T_N (7, 31), in region III so that the heavy-electron density of states at the superconducting transition at T_c is

$$N_f(\rho, T_c) = \frac{3 \ln 2}{2\pi^2 k_B T^*(\rho)} f_0(\rho) \left(1 - \frac{T_x(\rho)}{T^*(\rho)}\right)^{3/2} \left(1 + \ln \frac{T^*(\rho)}{T_x(\rho)}\right), \quad [8]$$

where $T_x(\rho) = T_L(\rho)$ in region I, $T_c(\rho)$ in region II, and $T_{0/N}(\rho)$ in region III (Fig. 2 C and D). Importantly, we see that because N_f varies inversely with T^* , the characteristic dimensionless pairing strength, $\kappa(\rho) = k_B T^*(\rho) N_f(\rho, T_c)$, depends comparatively weakly on T_x/T^* in all three regions:

$$\kappa(\rho) = \frac{3 \ln 2}{2\pi^2} \left(1 + \ln \frac{T^*(\rho)}{T_L(\rho)}\right), \quad (\text{region I}) \quad [9a]$$

$$\kappa(\rho) = \frac{3 \ln 2}{2\pi^2} f_0(\rho) \left(1 - \frac{T_c(\rho)}{T^*(\rho)}\right)^{3/2} \left(1 + \ln \frac{T^*(\rho)}{T_c(\rho)}\right), \quad (\text{region II}) \quad [9b]$$

$$\kappa(\rho) = \frac{3 \ln 2}{2\pi^2} f_0(\rho) \left(1 - \frac{T_0(\rho)}{T^*(\rho)}\right)^{3/2} \left(1 + \ln \frac{T^*(\rho)}{T_0(\rho)}\right). \quad (\text{region III}) \quad [9c]$$

Because $f(\rho_L, T_c^{\max}) = 1$, we find a simple formula for the maximal value of $\kappa(\rho)$ at ρ_L :

$$\kappa(\rho_L) = \frac{3 \ln 2}{2\pi^2} \left(1 + \ln \frac{T_m^*}{T_c^{\max}}\right). \quad [10]$$

Deducing Other Key Parameters from Experiment. The pressure dependence of the coherence temperature, $T^*(\rho)$, may be obtained from resistivity measurements (7, 19), and, in the case of Cd-doped CeCoIn₅, from Knight shift experiments (22). The results are shown in Fig. 2B, *Inset*.

To determine $f_0(\rho)$, we first note $f_0(\rho_{QC}) = 1$ and use experiment to determine f_0 at ambient pressure; for other pressures, we assume that $f_0(\rho)$ scales linearly with $T^*(\rho)$ (cf. ref. 11) and obtain

$$f_0(\rho) = 1 + (1 - f_0(0)) \frac{T^*(\rho) - T_{QC}^*}{T_{QC}^* - T^*(0)}, \quad [11]$$

where $f_0(0)$ is the hybridization parameter at ambient pressure and $T^*(0)$ and T_{QC}^* are the coherence temperatures at ambient pressure and the QCP, respectively.

For CeRhIn₅, one has $\rho_{QC} \sim 2.25$ GPa and $T_{QC}^* \sim 33$ K (18); an analysis of its magnetic properties yields $T^*(0) \sim 17$ K and $f_0(0) \sim 0.65$ at ambient pressure. For CeCoIn₅, a scaling analysis of the resistivity (20) suggests $\rho_{QC} \sim 1.1$ GPa and $T_{QC}^* \sim 82$ K, whereas an analysis of the temperature-magnetic field phase diagram yields $f_0(0) \sim 0.87$ and $T^*(0) \sim 56$ K at ambient pressure, a result that yields an excellent fit to the variation of the QCP with pressure (11). For Cd doping, we assume that 5% Cd doping has similar effect on f_0 as a negative pressure of -0.7 GPa, as is suggested by experiment (21). The effect of Cd doping is, however, different from pressurization because T^* is doping-independent, as is seen in the NMR experiment (22). For both materials, our choice of $f_0(\rho)$ leads to a unique prediction of $T_L(\rho)$ that can be verified experimentally.

The cutoff temperatures, $T_x(\rho)$, for the growth in the heavy-electron state density in region III are determined from the Knight shift and/or Hall measurements (7). For CeCo(In_{1-x}Cd_x)₅, experiment shows that T_x is roughly given by T_N ; for CeRhIn₅, experiment shows that $T_x = T_0 \sim 2T_N$ at ambient pressure and decreases to T_N at $\rho_N \sim 1.8$ GPa (7). In this region, a further experimental test of our choice of parameters is provided by the Néel temperature that can be calculated using Eq. 7.

On combining and inserting these experimental parameters into Eq. 9 we obtain the dimensionless pairing strength, $\kappa(\rho)$, in Fig. 2A and the results for T_N and T_c shown in Fig. 2 C and D that are in remarkably good agreement with experiment.

Prediction of a Dome-Like Structure for T_c . Our prediction of a dome-like structure for T_c versus pressure for any heavy-electron superconductor is based on the behavior of the solutions of Eq. 4 for the three distinct regions of emergent superconductivity.

Region I: $f_0 > 1$ and $T_c < T_L$. The growth of $N_f(T)$ is cut off at the delocalization temperature, T_L , below which $f(T) = 1$ and Eq. 4 only depends on f_0 ,

$$\frac{T_c}{T_c^{\max}} = \exp \left[-\lambda_{\max}^{-1} \left(\frac{1 + \ln(T_m^*/T_c^{\max})}{1 - \ln(1 - f_0^{-2/3})} - 1 \right) \right]. \quad [12a]$$

T_c is maximum at the pressure at which $T_c = T_L$; it decreases at higher pressures because the density of states decreases, being cut off at higher values of T_L by the increase in f_0 .

Region II: $f_0 \sim 1$ and $T_c > T_L$ and T_N . Because the growth of $N_f(T)$ extends to T_c , Eq. 4 takes the form

$$\frac{T_c}{T_c^{\max}} = \exp \left[-\lambda_{\max}^{-1} \left(\frac{1 + \ln(T_m^*/T_c^{\max})}{f_0(1 - T_c/T^*)^{3/2}(1 + \ln(T^*/T_c))} - 1 \right) \right] \quad [12b]$$

and has to be solved self-consistently. Most heavy-electron quantum critical superconductors fall in this region, where the logarithmically nearly divergent density of states acts to enhance the effective interaction by a factor, $[1 + \ln(T^*/T_c)]$, that can vary between 7.0 and 3.8 as one goes from $T_d/T^* = 0.0025$ to 0.062.

Region III: $f_0 < 1$ and $T_c < T_N$. The growth in N_F is cut off at T_0 so that

$$\frac{T_c}{T_c^{\max}} = \exp \left[-\lambda_{\max}^{-1} \left(\frac{1 + \ln(T_m^*/T_c^{\max})}{f_0(1 - T_0/T^*)^{3/2}(1 + \ln(T^*/T_0))} - 1 \right) \right]. \quad [12c]$$

With increasing pressure, f_0 increases and T_N and T_0 decrease, so that T_c increases and becomes greater than T_N before one reaches the quantum critical pressure.

A Consistency Check with Microscopic Strong Coupling Calculations. It is reasonable to assume that the pairing interaction for heavy-electron superconductivity is given by an expression identical to that used to explain quantum critical cuprate superconductivity (2),

$$V(\mathbf{q}, \omega) = g^2 \chi'(\mathbf{q}, \omega), \quad [13]$$

where g is the quasiparticle-spin fluctuation coupling strength and $\chi(\mathbf{q}, \omega)$, the dynamic susceptibility, follows the quantum critical form expected from its proximity to an antiferromagnetic state (13):

$$\chi(\mathbf{q}, \omega) = \frac{\chi_Q}{1 + (\mathbf{q} - \mathbf{Q})^2 \xi^2 - i\omega/\omega_{SF}}, \quad [14]$$

with a peak at the ordering wave vector, \mathbf{Q} , of magnitude $\chi_Q = \pi\chi_0(\xi/a)^2$, where ξ is the antiferromagnetic correlation length, a is the lattice constant, and χ_0 is the uniform spin susceptibility, and a temperature-dependent spin fluctuation energy, ω_{SF} . Because the measured ratios of the energy gap to T_c for heavy-electron materials are typically large compared with the weak coupling result, 1.75, any attempt to seek consistency between our proposed phenomenological expression for T_c and microscopic calculations should

begin with the strong coupling numerical results (14, 15) required to take account of the frequency dependence of the interaction, Eq. 13. Although these have yet to be carried out for heavy-electron materials, it is to be expected that these will yield a BCS-like expression in the strong coupling limit that is analogous to that found for the cuprates, namely,

$$T_c = \lambda_1 \omega_{SF} (\xi/a)^2 \exp \left(\frac{1}{\lambda_2 g N_F(T_c)} \right), \quad [15]$$

where λ_1 and λ_2 are constants of order unity.

The microscopic result, Eq. 15, will be consistent with our phenomenological expression, Eq. 1, if, first, the proposed microscopic prefactor, $\lambda_1 \omega_{SF} (\xi/a)^2$, is identical to $0.147 T_m^*$, the effective range over which we have proposed that the quantum critical spin fluctuation induced interaction will be attractive, and second, if the coupling, g , of the heavy-electron quasiparticles to the spin fluctuations scales with T^* , the nearest-neighbor local moment interaction (8). This last connection is plausible because through collective hybridization the heavy-electron quasiparticles are born coupled by an interaction similar to that of the local moments from which they emerge. Importantly, experimental information on the microscopic prefactor is available for CeColn₅, where neutron scattering measurements of the spin fluctuation spectrum near T_c at ambient pressure (23) yield $\omega_{SF} = 0.3 \pm 0.15$ meV and $\xi = 9.6 \pm 1.0$ Å (about twice the in-plane lattice constant $a = 4.60$ Å). One then has $\omega_{SF}(\xi/a)^2 = 1.3$ meV ~ 15.1 K, in remarkably close agreement with our phenomenological result, $0.147 T_m^* = 12.9$ K. The two expressions agree if we take $\lambda_1 = 0.85$ in Eq. 15 and assume that neutron scattering at the quantum critical pressure will yield results for this product that are similar to those found at ambient pressure. Future calculations and experiments on other materials can test our prediction that the microscopic prefactor will always be $\sim 0.147 T_m^*$.

ACKNOWLEDGMENTS. We thank G. Lonzarich for his critical reading and helpful comments on an earlier draft of this manuscript, Z. Fisk for his critical reading and helpful remarks about the framing of this manuscript, and the Aspen Center for Physics (National Science Foundation Grant PHY-1066293) and the Santa Fe Institute for their hospitality during its writing. Y.-f.Y. thanks the Simons Foundation for its support and this work is supported by National Natural Science Foundation of China Grant 11174339 and Strategic Priority Research Program (B) of the Chinese Academy of Sciences Grant XDB07020200.

- Mathur ND, et al. (1998) Magnetically mediated superconductivity in heavy fermion compounds. *Nature* 394(6688):39–43.
- Monthoux P, Pines D, Lonzarich GG (2007) Superconductivity without phonons. *Nature* 450(7173):1177–1183.
- Pines D (2013) Finding new superconductors: The spin-fluctuation gateway to high T_c and possible room temperature superconductivity. *J Phys Chem B* 117(42):13145–13153.
- Curro NJ, et al. (2005) Unconventional superconductivity in PuCoGa₅. *Nature* 434(7033):622–625.
- Yang Y-F, Pines D, Curro NJ (2014) Scaling and superconductivity in heavy electron materials. arXiv:1410.0452.
- Bardeen J, Cooper LN, Schrieffer JR (1957) Theory of superconductivity. *Phys Rev* 108(5):1175–1204.
- Yang Y-F, Pines D (2012) Emergent states in heavy-electron materials. *Proc Natl Acad Sci USA* 109(45):E3060–E3066.
- Yang Y-F, Fisk Z, Lee H-O, Thompson JD, Pines D (2008) Scaling the Kondo lattice. *Nature* 454(7204):611–613.
- Yang Y-F, Urbano R, Curro NJ, Pines D, Bauer ED (2009) Magnetic excitations in the kondo liquid: Superconductivity and hidden magnetic quantum critical fluctuations. *Phys Rev Lett* 103(19):197004.
- Yang Y-F, Pines D (2008) Universal behavior in heavy-electron materials. *Phys Rev Lett* 100(9):096404.
- Yang Y-F, Pines D (2014) Quantum critical behavior in heavy electron materials. *Proc Natl Acad Sci USA* 111(23):8398–8403.
- Nakatsuji S, Pines D, Fisk Z (2004) Two fluid description of the Kondo lattice. *Phys Rev Lett* 92(1):016401.
- Millis AJ, Monien H, Pines D (1990) Phenomenological model of nuclear relaxation in the normal state of YBa₂Cu₃O₇. *Phys Rev B* 42(1):167–178.
- Monthoux P, Pines D (1992) Spin-fluctuation-induced superconductivity in the copper oxides: A strong coupling calculation. *Phys Rev Lett* 69(6):961–964.
- Ueda K, Moriya T, Takahashi Y (1992) Antiferromagnetic spin fluctuations and high- T_c superconductivity. *J Phys Chem Solids* 53(12):1515–1521.
- Monthoux P, Lonzarich GG (2001) Magnetically mediated superconductivity in quasi-two and three dimensions. *Phys Rev B* 63(5):054529.
- Monthoux P, Lonzarich GG (2002) Magnetically mediated superconductivity: Cross-over from cubic to tetragonal lattice. *Phys Rev B* 66(22):224504.
- Park T, et al. (2006) Hidden magnetism and quantum criticality in the heavy fermion superconductor CeRhIn₅. *Nature* 440(7080):65–68.
- Nicklas M, et al. (2001) Response of the heavy-fermion superconductor CeColn₅ to pressure: Roles of dimensionality and proximity to a quantum-critical point. *J Phys Condens Matter* 13(44):L905–L912.
- Ronning F, et al. (2006) Pressure study of quantum criticality in CeColn₅. *Phys Rev B* 73(6):064519.
- Pham LD, Park T, Maquilon S, Thompson JD, Fisk Z (2006) Reversible tuning of the heavy-fermion ground state in CeColn₅. *Phys Rev Lett* 97(5):056404.
- Urbano RR, et al. (2007) Interacting antiferromagnetic droplets in quantum critical CeColn₅. *Phys Rev Lett* 99(14):146402.
- Stock C, Broholm C, Hudis J, Kang HJ, Petrovic C (2008) Spin resonance in the d-wave superconductor CeColn₅. *Phys Rev Lett* 100(8):087001.
- Muramatsu T, et al. (2003) Electrical resistivity of CeTln₅ (T=Rh, Ir) under high pressure. *Physica C* 388–389:539–540.
- Takaes Y, et al. (2011) Effect of pressure on transport properties of CeIrIn₅. *J Phys Conf Ser* 273(1):012058.
- Bauer ED, et al. (2012) Localized 5f electrons in superconducting PuColn₅: Consequences for superconductivity in PuCoGa₅. *J Phys Condens Matter* 24(5):052206.
- Tran VH, Kaczorowski D, Khan RT, Bauer E (2011) Superconductivity and non-Fermi-liquid behavior of Ce₂PdIn₈. *Phys Rev B* 83(6):064504.
- Chen G, et al. (2002) Observation of superconductivity in heavy-fermion compounds of Ce₂Coln₈. *J Phys Soc Jpn* 71(12):2836–2838.
- Knebel G, Braithwaite D, Canfield PC, Lapertot G, Flouquet J (2001) Electronic properties of CeIn₃ under high pressure near the quantum critical point. *Phys Rev B* 65(2):024425.
- Trappmann T, Löhneysen Hv, Taillefer L (1991) Pressure dependence of the superconducting phases in UPT₃. *Phys Rev B Rapid Commun* 43(16):13714–13716.
- Shirer KR, et al. (2012) Long range order and two-fluid behavior in heavy electron materials. *Proc Natl Acad Sci USA* 109(45):E3067–E3073.